ACS OMEGA

http://pubs.acs.org/journal/acsodf

Article

Fissure Grouting Mechanism Accounting for the Time-Dependent Viscosity of Silica Sol

Weijie Zhang, Fei Yang, Chenghao Han,* Qian Ren, Ziyu Peng, Fangxiao Wu, and Zhenyong Zhang

Cite This: *ACS Omega* 2021, 6, 28140−28149

Read Online

ACCESS | Metrics & More | Article Recommendations

ABSTRACT: Subject to the complex hydrogeological environment where underground engineering is located, the grouting prevention and control of microfissure water ingress are increasingly strict. Silica sol grout has been increasingly used in field tests because of its fine particles and good injectability. Therefore, it is necessary to examine the time-dependent viscosity of silica sol grout and clarify its diffusion law in a rock fissure. In this study, the time dependence of the viscosity of silica sol grout was studied, and then the grout viscosity was subdivided into a slow growth period, accelerated growth period, and rapid curing period according to the growth rate. The effects of the concentration of colloidal silica suspension, the concentration of accelerant, and the mixing volume ratio of the two on the growth of the slurry viscosity were studied. A parameter λ was introduced to comprehensively characterize the influence of the three factors on the rheological properties of the slurry. The relationship between the gel induction time and λ and the accelerating growth stage of the slurry gel was obtained by data fitting. The time-dependent equation of the silica sol solution was established. The difference in the grouting diffusion law between silica sol grout and cement−sodium silicate grout (C-S grout) is compared and analyzed by a stepwise calculation method under two grouting modes (constant-pressure grouting and constant-rate grouting). The results show that under the condition of constant-pressure grouting, the silica sol grout migrates and diffuses continuously for a long time, while the C-S grout is close to the final diffusion form at 15−20 s, and the maximum diffusion distance is much smaller than that of silica sol grout. Under the condition of constant-rate grouting, the grouting pressure driving C-S grout increases sharply with time. Compared with C-S grout, silica sol grout has the obvious advantages of a longer effective diffusion time and lower energy consumption. The research results have certain theoretical significance and reference value for the engineering design of silica sol grouting.

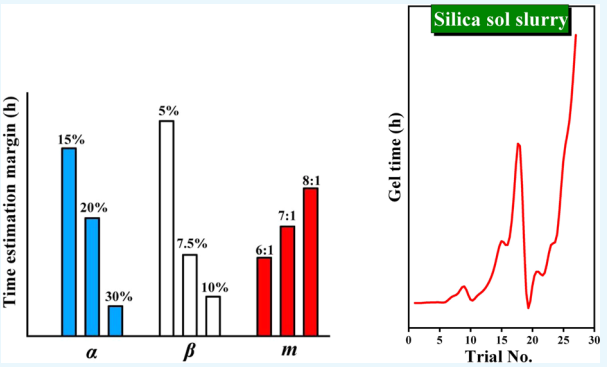

1. INTRODUCTION

Fissures have a tendency to increase the permeability of a rock mass.[1,2] While water-bearing fissures are encountered in underground engineering, large amounts of water can be released, which can cause casualties and significant property losses. Since the grouting technique was invented, this method has been extensively applied to improve the performance of rock masses and to seal against water ingress in underground construction.[3,4]

At present, underground engineering construction is facing more complex hydrogeological conditions, which puts forward higher requirements for groundwater control.[5] In some cases, traditional cement grout using standard methods fails to seal the fissures to an acceptable level.[6] For example, nanoscale fissures need to be sealed in the construction of geological disposal facilities for nuclear waste, and during the construction of traffic tunnels under sea, lake, river, and other water bodies, to reduce the leakage from above, it is necessary to block the microcracks in the rock mass as much as possible.[7−11] The minimum fissures aperture that traditional suspensions (such as cement slurry, ultrafine cement slurry, and cement−sodium silicate slurry) can penetrate is approximately 50−100 μm, and the permeability coefficient of the injection part is 10^{-1}−10^{-2} cm/s. The nano/microfissures and low-permeability strata cannot be effectively grouted, which leads to poor sealing of rock fissures and large residual water inflow after grouting.[12−16] Hence, the demand for grouting sealing of microcracks urges people to turn to nanoslurry represented by silica sol. Silica sol is the dispersion of nanosized SiO_2 particles in water. The molecular formula can be expressed as $mSiO_2{\cdot}nH_2O$, which is a colloidal solution.[17] Silica sol has an electric double-layer structure.

Received: August 6, 2021
Accepted: September 30, 2021
Published: October 13, 2021

(a) (b)

Figure 1. Test instrument: (a) NDJ-9S rotary-type viscometer and (b) JB300-SH digital constant blender.

When ionic Na or Ca is added, the electric double layer becomes thinner and the silica particles connect to form a gel.[18] Therefore, as a kind of gel-controllable slurry, silica sol slurry can achieve gel action when silica sol solution is mixed with an accelerating agent. The gelation time can be controlled by changing the temperature, concentration of silica sol solution, and dosage of the accelerator.[19]

Theory and practice show that gel-controllable grouts, such as traditional cement−sodium silicate slurry and silica sol, are effective materials for grouting treatment of fractured rock masses. Silica sol slurry acts in the same way as a Newtonian liquid. It thus has no yield shear strength and will still flow as long as there is a pressure gradient.[6] In recent years, some scholars have researched grouting theory and engineering applications of gel-controllable grout. Liu et al. carried out a series of laboratory tests on the diffusion of fast setting slurry and summarized the diffusion law of cement−sodium silicate grout in flat fissures.[20] Li et al. studied the time-dependent characteristics of the viscosity of cement−sodium silicate grout and established a time-dependent equation.[21] Zhang et al. obtained the distribution characteristics of the viscosity of rapidly setting cement-based grout in the process of fissures grouting in time and space.[22] Zhang deduced the diffusion control equation of the time-dependent behavior of cement-based slurry in fissures under still water conditions and discussed the control factors of the slurry diffusion process.[23] Sui et al. studied the process of dynamic water grouting for horizontal fissures and analyzed the influencing factors of chemical grout in dynamic water plugging.[24] Wang et al. investigated the effects of temperature and accelerant concentration on the gel time of silica sol slurry, and the relation between the real-time consistency of silica sol and the real-time penetration length was described.[25,26] Shen et al. found that the logarithm of the sol−gel time of silicon depends on the concentration of the accelerant.[27] Funehag et al. established a prediction model of the one-dimensional flow of silica sol slurry in microcracks (40−50 μm wide).[28] To explore the slurry diffusion process in fissures, Kim et al. proposed a method to predict the diffusion form of cement-based slurry with time-varying viscosity in porous media.[29] Mohajerani et al. proposed a grouting pressure calculation method considering the variation in the time of the grout viscosity and predicted the diffusion distance of grout in fissures.[30] Zhang et al. carried out a theoretical study of fissures grouting using the stepwise calculation method and analyzed the diffusion process of flat fissures considering the time- and space-dependent slurry viscosity.[31] Wei et al. used the improved stepwise calculation method to simulate the slurry diffusion of silica sol slurry in a single fissure and addressed the slurry diffusion rule under the dynamic parameter grouting mode and the time-varying characteristics of the slurry viscosity.[2,32] Ming Tian prepared a silica sol-modified cement grout that can seal engineering cracks of deep geological disposal.[33]

The above research is of great importance for understanding the conventional fissures grouting diffusion mechanism of gel-controllable grout, especially cement−sodium silicate slurry. However, for the design of microfracture grouting engineering, the limitations of existing research cannot be ignored. One of the reasons is that there is a lack of research on the gel mechanism and diffusion law of colloidal slurry represented by silica sol. The main objective of this paper is to study the influencing factors and time dependence of the viscosity of silica sol slurry via a laboratory investigation. In this study, the concentration of colloidal silica, the concentration of accelerators, and the volume mixing ratio were considered. The time-dependent equation of slurry viscosity was established, and the quantitative relationship between the slurry ratio parameters and slurry gel time was proposed. Then, the fissures grouting process of silica sol grout and cement-based grout was investigated using the improved stepwise calculation method. The variation characteristics of the grouting pressure and diffusion distance with grouting time were explained with different time-dependent viscosity grout types. The research results are expanded to provide references for the engineering design of silica sol grouting.

2. RESULTS

2.1. Rheology of Silica Sol Grout. Three main factors, including the concentration of colloidal silica suspension (α), the concentration of NaCl solution (β), and the mixing volume ratio (m) of colloidal silica suspension and NaCl solution, were selected in this study. In the experiment, α = 15, 20, and 30%,

https://doi.org/10.1021/acsomega.1c04216
ACS Omega 2021, 6, 28140−28149

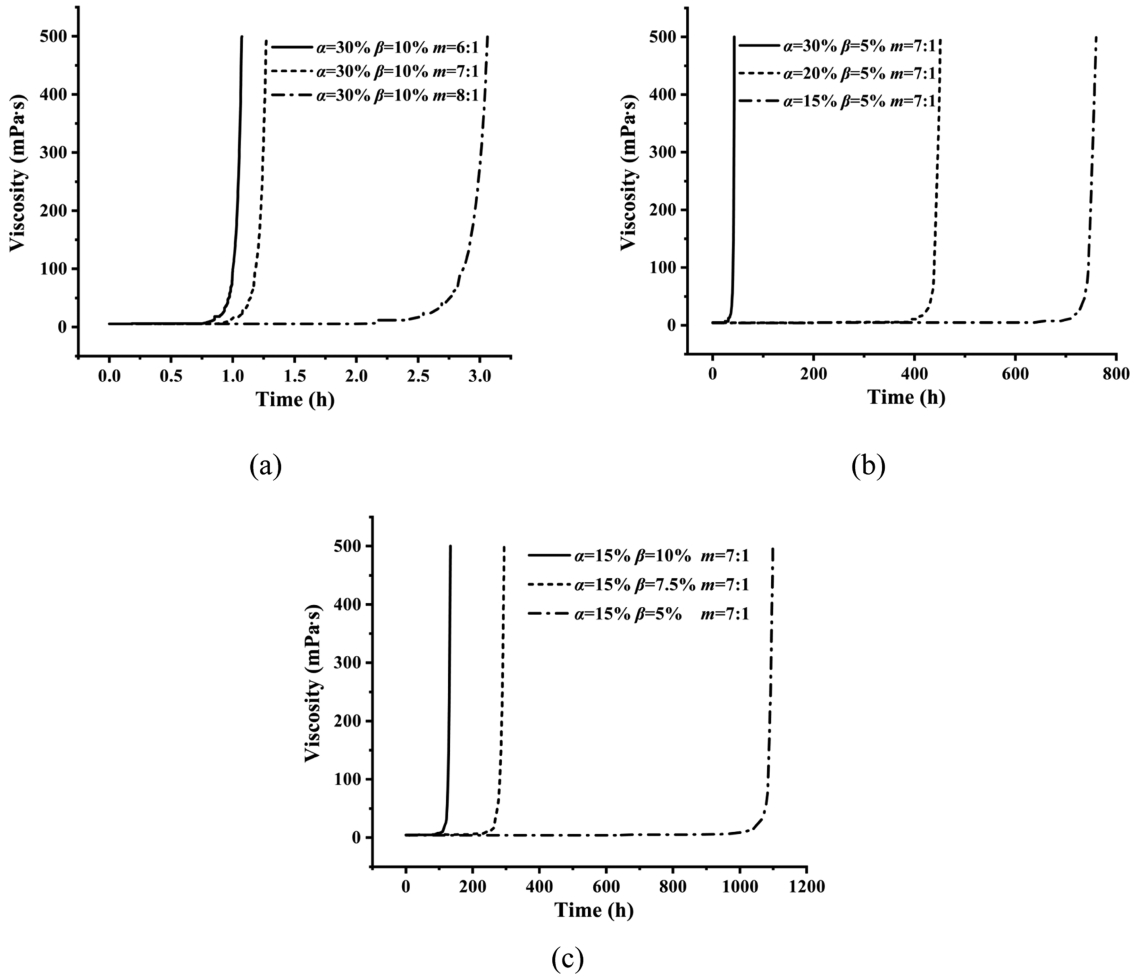

Figure 2. Grout viscosity with time after the addition of the accelerator. (a) Effect of m on viscosity. (b) Effect of α on viscosity. (c) Effect of β on viscosity.

β = 5, 7.5, and 10%, and m = 6:1, 7:1, and 8:1, respectively. The changes in the viscosity of silica sol slurry with mixing time under the influence of α, β, and m were measured by a viscometer and a blender (Figure 1). It is generally recognized that after the viscosity of silica sol grout reaches 100 mPa·s, the grout enters the gel stage, and the time required for the viscosity of silica sol grout to reach 100 mPa·s is defined as the gel time.[34] To investigate the influence of various factors on the slurry gel process, some typical change curves are obtained in Figure 2.

Figure 2a shows the effect of mixing volume ratio m on the time-dependent behavior of the viscosity of silica sol grout under the conditions of α = 30% and β = 10%. Figure 2a shows that the gel time of silica sol grout is positively correlated with the mixing volume ratio, and the gel time extends with increasing mixing volume ratio from 1.00 to 2.67 h. Figure 2b describes the effect of the concentration of colloidal silica suspension α (15−30%) on the time-dependent behavior of slurry viscosity under the condition of β = 10% and m = 7:1. When the concentrations of α were set to 15, 20, and 30%, the gel times were 742.92, 439.03, and 40.33 h, respectively. This suggests that the gel time of the slurry decreases with increasing α. Figure 2c shows the effect of the concentration of NaCl solution β (5−10%) on the time-dependent behavior of the viscosity of silica sol under the condition of α = 15% and m = 8:1. The analysis demonstrates that the gel time is negatively correlated with the mixing volume ratio and the increase in NaCl concentration significantly reduces the gel time. When the concentrations of silica sol are 5, 7.5, and 10%, the gel times of the slurry are 1083.26, 280.77, and 126.30 h, respectively.

Silica sol has an electric double-layer structure. When ionic sodium is added, the electric double layer becomes thinner, and the silica particles are connected to form a gel.[18] The concentration of colloidal silica suspension (α), concentration of NaCl solution (β), and mixing volume ratio (m) affect the gel time of silica sol slurry by controlling the concentration of SiO_2 and Na^+ in the slurry after mixing. Increases in α and β lead to increases in SiO_2 concentration and Na^+ concentration in the slurry, respectively. Na^+ is more likely to contact SiO_2 and react with SiO_2, thus accelerating the slurry gel. The increase in m led to a decrease in Na^+ concentration, which slowed the effect on SiO_2 agglomeration and led to an increase in gel time.

In Figure 2, the initial viscosity and end time of the silica sol slurry in each group of experiments are different from others. However, this figure demonstrates that all colloidal silica grouts exhibit high viscosity over time. The viscosity of the slurry maintains a slowly increasing trend for a long time after mixing. When the mixing time exceeds a certain point, the growth rate of the slurry viscosity gradually increases with time until it grows rapidly at a relatively stable rate and turns into a solid

https://doi.org/10.1021/acsomega.1c04216
ACS Omega 2021, 6, 28140−28149

state. Accordingly, the changes in the viscosity of silica sol slurry can be divided into three stages: a slow growth period, an accelerated growth period, and a rapid curing period, as shown in Figure 3. During the slow growth period, the slurry

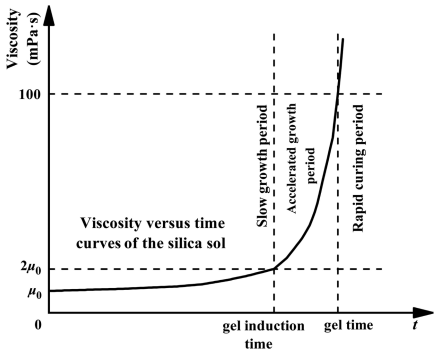

Figure 3. Schematic diagram of silica sol grout viscosity periods.

viscosity was low and grew slowly. The duration was approximately 90% of the entire experiment time. The time at which the viscosity doubles is designated the gel induction time.[6] After the gel induction time is reached, the slurry viscosity enters the accelerated growth period, and the growth rate of the slurry viscosity gradually accelerates until the slurry begins to gel. Then, the slurry enters the rapid curing stage, where the viscosity rises rapidly and the slurry thickens rapidly until solidification. At this stage, the slurry changes from fluid state to solid state and finally loses fluidity. When the viscosity reaches a maximum of 500 mPa·s, the experiment is stopped.

The contribution of α, β, and m to the growth of slurry viscosity was studied by variance analysis. Table 1 shows the

Table 1. Analysis of the Variance Results

factors	F	P
α	10.732	<0.001
β	14.431	<0.001
m	2.071	0.053

results of the variance analysis of the factors in this experiment. In Table 1, F is a statistic of the F-distribution, which describes the importance of factors, and P is used to indicate significance. When P is between 0.01 and 0.05, the difference is significant; when P is less than 0.01, the difference is extremely significant; and when P is greater than 0.05, the difference is not significant. The influences of the factors are ranked in the order of decreasing effect as follows: concentration of NaCl solution, concentration of silica sol solution, and mixing volume ratio.

2.2. Time-Dependent Equation of Viscosity. While the viscosity of silica sol increases slowly, the slurry does not have difficulty flowing and diffusing in porous media. Once the viscosity growth enters the acceleration stage, the slurry viscosity resistance increases and has great antidispersion ability, which is enough to resist a certain degree of hydrodynamic pressure. Therefore, the accelerated growth period is the key stage to block the water inflow channel of microfractures.

The gel induction time T_0 and the start and end times of the accelerated growth period of slurry viscosity obtained in the experiment are shown in Table 2. An equation that describes the viscosity growth is

$$\mu(t) = \exp(at^2 + bt + c) \tag{1}$$

where t is the slurry mixing time; $\mu(t)$ is the slurry viscosity at time t; and a, b, and c are the fitting constants, which are affected by the concentration of colloidal silica suspension, the concentration of the accelerant, and the mixing volume ratio.

To comprehensively analyze the influence of various experimental factors on the time-dependent behavior of the viscosity of silica sol slurry, a comprehensive characterization parameter λ was introduced in this study, as shown in eq 2

$$\lambda = \frac{m}{\alpha\beta} \tag{2}$$

where α is the concentration of colloidal silica suspension, β is the concentration of NaCl solution, and m is the mixing volume ratio.

Figure 4 presents λ versus gel induction time (T_0) and duration of the accelerated growth period (T_1) curves of the silica sol grout.

Figure 4a shows that under experimental conditions, T_0 is positively correlated with λ. With increasing λ, T_0 increases from 0.83 h to 976 h and the expressions of the relationship between them are as follows

$$T_0 = 0.0014\lambda^2 - 0.6086\lambda + 57.672 \tag{3}$$

where T_0 is the gel induction time under any λ and the correlation coefficient (R^2) is 0.966.

Figure 4b shows that T_1 is positively correlated with T_0. With increasing T_0, T_1 increases from 0.17 to 107.26 h, and the relationship between them is expressed as follows

$$T_1 = 0.3269T_0^{0.8481} \tag{4}$$

where T_1 is the duration of accelerated growth and the correlation coefficient R^2 is 0.941.

Thus, eqs 3 and 4 are combined, and the relationship between λ and T_1 can be obtained as follows

$$T_1 = 0.3269(0.0014\lambda^2 - 0.6086\lambda + 57.672)^{0.8481} \tag{5}$$

Equations 3−5 indicate that both the gel induction time and the duration of accelerated growth of the silica sol slurry can be expressed as a function of the comprehensive characterization parameter λ. Therefore, in a specific grouting case, according to the requirements of engineering grouting, the time range of the grout gel can be determined. Then, the λ value can be controlled by adjusting the concentration of colloidal silica suspension, the concentration of NaCl solution, and the mixing volume ratio between the two so that the λ value can meet the scope of grouting requirements.

2.3. Diffusion Law of Fast Curing Grout in Fissure. The theoretical analysis of fissure grouting diffusion of silica sol grout and C-S grout is based on the Newtonian fluid hypothesis. The diffusion governing equation is

$$\frac{dp}{dr} = \frac{3q\mu(t)}{4\pi r b^3} \tag{6}$$

where p is the grouting pressure, r is the slurry diffusion distance, q is the grouting rate, b is the fissure width, and $\mu(t)$ is a time-dependent function of the slurry viscosity.

The equations of the time-dependent behavior of the viscosity were used for silica sol slurry during the accelerated growth period, and Zhang proposed the time-dependent equation for the C-S slurry.[23]

https://doi.org/10.1021/acsomega.1c04216
ACS Omega 2021, 6, 28140−28149

Table 2. Parameters of Each Stage of Silica Gel

trial	initial viscosity (mPa·s)	gel induction time T_0 (h)	accelerated growth period (h)	viscosity time-dependent equation of accelerated growth period
1	5.4	0.83	0.83−1.00	$\mu(t) = \mathrm{Exp}(33.6008 - 77.8550t + 48.7438t^2)$
2	5.4	0.98	0.98−1.16	$\mu(t) = \mathrm{Exp}(36.1007 - 51.8184t + 28.3675t^2)$
3	5.4	2.17	2.17−2.87	$\mu(t) = \mathrm{Exp}(26.5438 - 21.8913t + 4.9642t^2)$
4	5.5	2.79	2.79−3.50	$\mu(t) = \mathrm{Exp}(29.7765 - 19.7294t + 3.5717t^2)$
5	5.5	2.84	2.84−3.72	$\mu(t) = \mathrm{Exp}(22.8337 - 14.3885t + 2.5461t^2)$
6	5.2	4.34	4.34−5.30	$\mu(t) = \mathrm{Exp}(41.2027 - 18.2324t + 2.1378t^2)$
7	5	20.75	20.75−26.08	$\mu(t) = \mathrm{Exp}(23.6482 - 2.1346t + 0.0539t^2)$
8	4.8	30.75	30.75−40.33	$\mu(t) = \mathrm{Exp}(29.1192 - 1.6898t + 0.0268t^2)$
9	5.3	46.5	46.5−67.15	$\mu(t) = \mathrm{Exp}(7.9229 - 0.1989t + 0.0021t^2)$
10	4.5	9.75	9.75−14.50	$\mu(t) = \mathrm{Exp}(50.9909 - 8.4829t - 0.3646t^2)$
11	4.2	24.5	24.5−28.23	$\mu(t) = \mathrm{Exp}(33.9618 - 2.9536t + 0.0677t^2)$
12	4.5	42.5	42.5−49.20	$\mu(t) = \mathrm{Exp}(44.0180 - 2.0936t + 0.0262t^2)$
13	4.2	75	75−86.80	$\mu(t) = \mathrm{Exp}(82.6336 - 2.1408t + 0.0143t^2)$
14	4.3	127	127−159.91	$\mu(t) = \mathrm{Exp}(74.6351 - 1.0679t + 0.0039t^2)$
15	4.5	203	203−250.57	$\mu(t) = \mathrm{Exp}(91.6666 - 0.8312t + 0.0019t^2)$
16	4.4	217	217−237.05	$\mu(t) = \mathrm{Exp}(486.4923 - 4.3713t + 0.0099t^2)$
17	4.2	389	389−439.03	$\mu(t) = \mathrm{Exp}(182.2791 - 0.9082t + 0.0012t^2)$
18	4.1	584	584−629.04	$\mu(t) = \mathrm{Exp}(447.4533 - 1.5.66t + 0.0013t^2)$
19	4.4	33	33−39.82	$\mu(t) = \mathrm{Exp}(72.8369 - 4.1765t - 0.0618t^2)$
20	4.3	63	63−71.33	$\mu(t) = \mathrm{Exp}(27.9063 - 0.9997t - 0.0094t^2)$
21	4.3	104	104−126.30	$\mu(t) = \mathrm{Exp}(86.4195 - 1.5601t - 0.0072t^2)$
22	4.1	114	114−124.47	$\mu(t) = \mathrm{Exp}(26.9329 - 0.6078t + 0.0034t^2)$
23	4	184	184−235.49	$\mu(t) = \mathrm{Exp}(188.7574 - 1.7585t + 0.00415t^2)$
24	4.6	234	234−280.77	$\mu(t) = \mathrm{Exp}(59.6382 - 0.4997t + 0.0011t^2)$
25	4.1	533	533−578.64	$\mu(t) = \mathrm{Exp}(395.3177 - 1.4605t + 0.0014t^2)$
26	4.1	704	704−742.92	$\mu(t) = \mathrm{Exp}(396.7449 - 1.1395t - 0.0008t^2)$
27	4.1	976	976−1083.26	$\mu(t) = \mathrm{Exp}(357.0312 - 0.705t + 0.0004t^2)$

By comparing the fissures grouting process of silica sol and C-S slurry under different conditions, the curve between the injection time and penetration length is drawn, as shown in Figures 5 and 6. Then, the influence of fissure width and grouting pressure on fissures grouting could be examined in detail.

As shown in Figure 5, the diffusion distance of the slurry changes greatly between different fissure widths when the grouting pressure is 9000 Pa. The real-time penetration length of silica sol increases with increasing injection time, but the growth rate decreases slowly. The slurry can be in a state of effective diffusion for a long time in fissures. In contrast, the diffusion rate of the C-S slurry decreases rapidly in flat fissures. The maximum effective diffusion distance is reached at approximately 20 s, after which diffusion almost stops. In other words, the effective diffusion time of the C-S slurry in fissures is limited in the process of constant-pressure grouting. At the same fissure width, the diffusion distance of silica sol grout in flat fissures is always larger than that of C-S grout, and the gap grows with increasing injection time.

Figure 6 describes the changes in the diffusion distance between different grouting pressures with the same fissure width. The diffusion law of different grout types in the slab fissures is similar to that in Figure 5.

Figures 5 and 6 show that grouting pressure and fissure width have significant effects on the slurry diffusion distance. The curves for the grouting pressure and fissure width with varying grouting diffusion distance in 60 s (i.e., final diffusion distance of grouting) were drawn, and the influences of the fissure width (b) and grouting pressure (p) on the grouting diffusion were analyzed.

As shown in Figure 7, the formula for the slurry diffusion distance with the fissure width and grouting pressure was established. Figure 7a shows that the ultimate diffusion distance of both types of grout increases linearly with fissure width. When the grouting pressure is constant at 9000 Pa and the fissure width is 0.5 mm, the final diffusion distances of silica sol grout and C-S grout are 0.82 and 0.40 m, respectively. When the fissure width is 2.0 mm, the final diffusion distance of silica sol grout is 2.95 m and the final diffusion distance of C-S grout is 1.47 m. When the grouting pressure is constant, the final diffusion distances of the two grout types are obviously different and the silica sol grout is approximately twice that of the C-S grout. Figure 7b describes the power function relationship between the final diffusion distance of the two kinds of grout and grouting pressure. When the fissure width is 2.0 mm and the grouting pressure is 5000 Pa, the final diffusion distance of silica sol grout is 2.23 m and the final diffusion distance of C-S grout is 1.10 m. Under the condition of a grouting pressure of 25 000 Pa, the final diffusion distance of silica sol grout is 4.85 m, and the final diffusion distance of C-S grout is 2.42 m. When the fissure width is constant, the final diffusion distance of silica sol grout is obviously larger than that of C-S grout and is always twice that of C-S grout.

In summary, under the condition of constant-pressure flat fissures grouting, the diffusion rates of both silica sol grout and C-S grout decrease with increasing grouting time, but the latter decreases more strongly. Finally, the diffusion rate of C-S grout in cracks decreases rapidly, reaching the limit value around 15−20 s. The "effective diffusion" time is very limited, and the diffusion distance has a significant limit. In contrast, the time-effective diffusion of silica sol slurry is much longer and the final diffusion distance can be larger in the fissures.

https://doi.org/10.1021/acsomega.1c04216
ACS Omega 2021, 6, 28140−28149

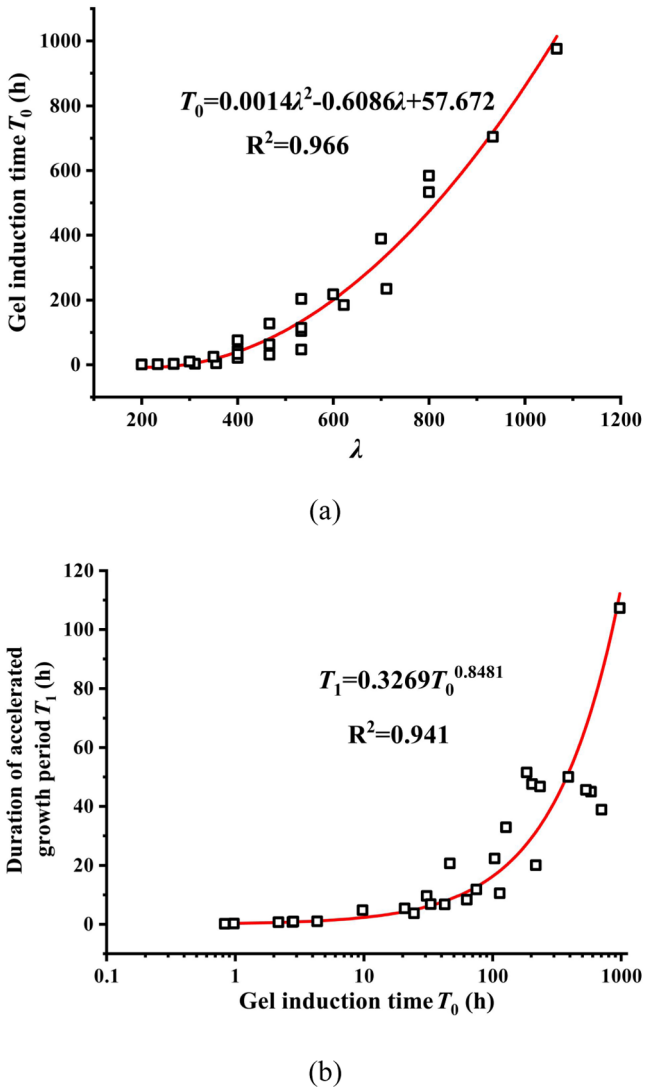

Figure 4. Fitting curves of experimental factors on gel induction time. (a) Impact of λ on T_0. (b) Impact of T_0 on T_1.

Figure 8 describes the pressure distribution in the diffusion zone of grouting at 20, 40, and 60 s. The pressure value of the C-S slurry in the diffusion region decreases with increasing diffusion distance, and the decreasing rate increases. The pressure at the hole increases sharply with the progress of grouting, and the maximum pressure at the hole is 25 688 Pa for 60 s. The pressure value of the silica sol slurry in the diffusion region also decreases with the increase in the diffusion distance, but the decreasing rate decreases continuously, and the pressure near the injection hole increases slowly with the progress of grouting. At the end of grouting, the pressure at the hole was 716 Pa, which was only 1/36 that of the C-S slurry and was much smaller than that of the C-S slurry.

Therefore, when the same grouting rate is selected, the pressure and its distribution in the grouted zone are remarkably different due to the variation in slurry rheology. Furthermore, as the designed penetration length is selected to be the same, the energy consumed by the C-S slurry is much greater than that of silica gel; that is, the latter is better than the former, which is injected into the fissure, especially the microfissure.

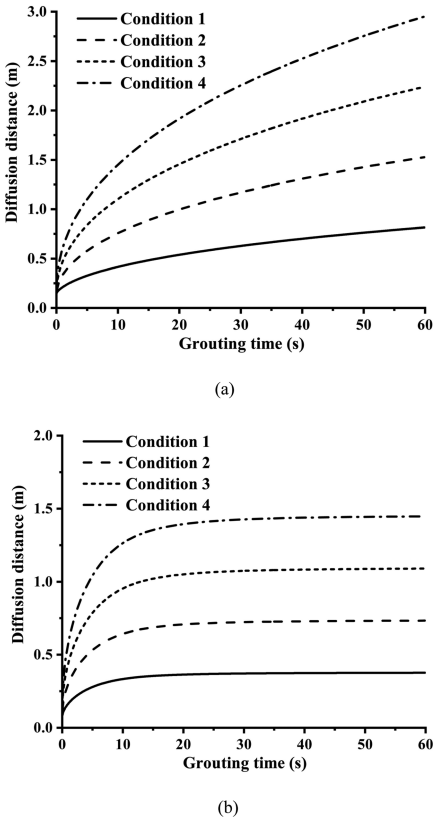

Figure 5. Curve of the diffusion distance of the slurry with time under different fissure widths. (a) Silica sol slurry. (b) C-S slurry.

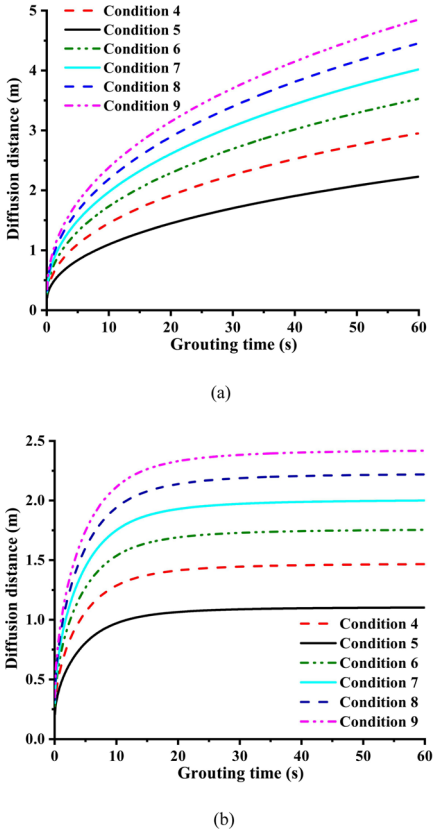

Figure 6. Time-varying curve of slurry diffusion distance under different grouting pressures. (a) Silica sol slurry. (b) C-S slurry.

https://doi.org/10.1021/acsomega.1c04216
ACS Omega 2021, 6, 28140−28149

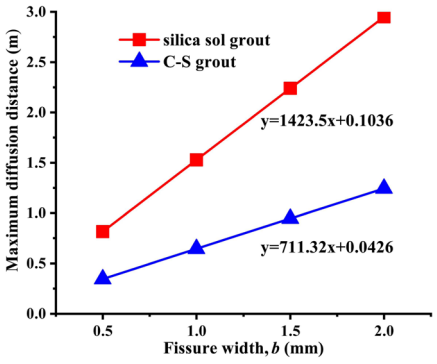

(a)

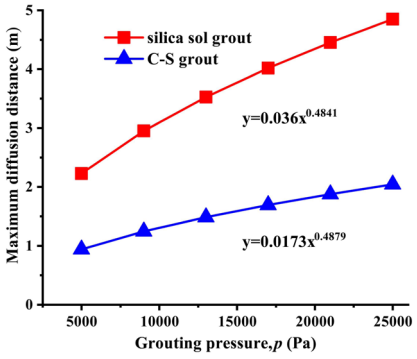

(b)

Figure 7. Curve of the diffusion distance of the slurry under constant pressure. (a) Different fissure widths. (b) Different grouting pressures.

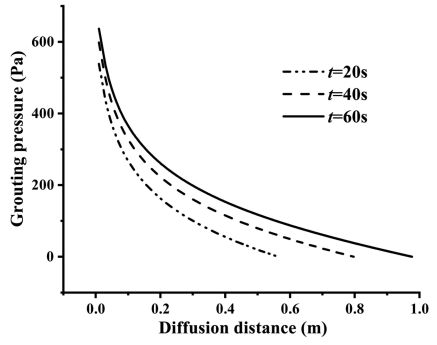

(a)

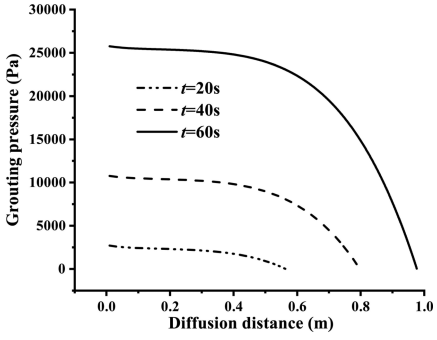

(b)

Figure 8. Spatial distribution of the slurry pressure at different times under grouting flow rate boundary conditions. (a) Silica sol slurry. (b) C-S slurry.

3. DISCUSSION

Compared with cement-based grout, the particles in silica sol grout belong to the nanometer level and have better injectability, which is more than enough to meet the engineering needs to block the water gushing originating from microfissures. Therefore, the study of the basic properties of silica sol grout and its diffusion law in fissures has a certain guiding significance for grouting engineering design. Under different slurry ratios, the viscosity of silica sol slurry varies significantly. The concentration of the silica sol solution, accelerator concentration, and mixing ratio all have an important impact on the rheology of the slurry. In this paper, a comprehensive characterization parameter λ is therefore proposed to describe the association of three factors on the gel time of the slurry. The relationship equation between λ and the gel induction time and the length of the accelerated growth period of the viscosity is given. In the practice of grouting engineering, design parameters such as the injection borehole spacing can be identified according to the engineering geological conditions in the study area. Then, the duration interval of the required accelerated growth period of the slurry is calculated and the range of the comprehensive characterization parameter λ is determined. Finally, under the guidance of parameter λ, the concentration of colloidal silica suspension, the concentration of the accelerant, and the mixing ratio are dynamically adjusted to prepare the silica sol slurry, which meets the practical needs of engineering.

After the silica sol grout is mixed, there exists a long period of low viscosity, during which the grout penetration ability is strong. In actual grouting engineering, this stage should be used to allow the grout to fully diffuse. When the slurry viscosity increases to the accelerated stage, the viscosity increases dramatically, which is the key period for fissure grouting to seal the water inrush. Compared to traditional cement-based quick-setting grout such as C-S grout, the viscosity of silica sol grout experienced a much longer time in the slow growth stage and the accelerated growth stage. Therefore, the silica sol slurry can promote the slurry diffusion farther. That is, with a small number of grouting holes, the hydraulic needs of a larger range of fissure grouting plugging can be met. At the same time, the energy consumption of silica sol grout injection is much smaller than that of C-S grout, which has prominent advantages in the practice of grouting engineering.

In this paper, the effect of the ratio of the slurry on the time-varying viscosity of the silica sol slurry was studied. However, the influence of the chemical field and temperature field of groundwater has not been considered. In the future, research on the influence of environmental factors on the rheological properties of grout, the long-term grouting efficiency of silica sol grout, and the anti-erosion ability of grout will be planned. This is supposed to have a more meaningful guiding effect on actual grouting engineering.

4. CONCLUSIONS

In this study, the time-dependent behavior of the viscosity of silica sol slurry was revealed. The viscosity changing process of the silica sol slurry was divided into three stages, namely, the slow growth period, the accelerated growth period, and the rapid curing period. Generally, the viscosity increases slowly for a long time after mixing and rapidly increases to the final gel in a short time after entering the acceleration period. The

https://doi.org/10.1021/acsomega.1c04216
ACS Omega 2021, 6, 28140−28149

Table 3. Experimental Design Parameters of the Time-Varying Viscosity of Silica Sol

trial	concentration of colloidal silica suspension, α (%)	concentration of NaCl solution, β (%)	mixing volume ratio, m	trial	concentration of colloidal silica suspension, α (%)	concentration of NaCl solution, β (%)	mixing volume ratio, m
1	30	10	6:1	15	20	7.5	8:1
2	30	10	7:1	16	20	5	6:1
3	30	10	8:1	17	20	5	7:1
4	30	7.5	6:1	18	20	5	8:1
5	30	7.5	7:1	19	15	10	6:1
6	30	7.5	8:1	20	15	10	7:1
7	30	5	6:1	21	15	10	8:1
8	30	5	7:1	22	15	7.5	6:1
9	30	5	8:1	23	15	7.5	7:1
10	20	10	6:1	24	15	7.5	8:1
11	20	10	7:1	25	15	5	6:1
12	20	10	8:1	26	15	5	7:1
13	20	7.5	6:1	27	15	5	8:1
14	20	7.5	7:1				

time-dependent viscosity of the slurry during the accelerated growth period is in the form of a power exponential function. The viscosity function of the chemical reaction time fitted in this paper can accurately describe the viscosity variation characteristics of the slurry during the acceleration period.

The concentration of the colloidal silica suspension, the concentration of the accelerant, and the mixing ratio all affect the time-varying viscosity of the silica sol slurry. The comprehensive characterization parameter λ was put in place to characterize the correlation of the three indexes on the gel time of the slurry. Based on data fitting analysis, the relationship equation between the inclusive characterization parameter λ and the gel induction time and the length of the accelerated growth period was obtained. This paper guides the systematic optimization of the ratio of grout in practical engineering.

The diffusion process of silica sol grout and C-S grout in horizontal fissures under constant-pressure and constant-rate grouting conditions was studied using a stepwise calculation method. The influence of the grouting pressure, fissure aperture, and grouting rate on the rate of change of the diffusion distance and the final diffusion range of different grout is analyzed. Compared with C-S grout, silica sol grout has a longer effective diffusion time and a larger diffusion distance under constant-pressure grouting conditions. Under the condition of constant-rate grouting, a smaller grouting pressure is needed to inject silica sol grout into the fissure.

5. EXPERIMENTAL PROCEDURES

5.1. Materials. The selected grout solutions consisted of a colloidal silica suspension and an accelerator. Colloidal silica contains 40% silica solids by weight. The colloidal silica suspension before the addition of the accelerator had a pH of 9.3, a density of 1290 kg/m^3, and a dynamic viscosity of 26 mPa·s. Different concentrations of colloidal silica suspensions can be prepared by mixing distilled water. The accelerator was prepared by mixing different qualities of analytically pure NaCl particles with 1 kg of purified water. The accelerator had a neutral pH of 7 and a dynamic viscosity of 1.10 mPa·s.

5.2. Experimental Setup. The experimental setup for investigating the time-dependent behavior of the viscosity of silica sol slurry is shown in Figure 1. It includes an NDJ-9S rotary-type viscometer, a JB300-SH digital constant blender, and a computer. The range of the viscometer is 1−500 mPa·s, and the division value is 0.1 mPa·s, and the viscometer can directly measure the data for the change in the apparent viscosity of silica sol slurry with mixing time. Due to the limitation of the current developmental level of fluid viscosity measurement technology, only the change in apparent viscosity with time can be measured for a slurry with a viscosity that increases significantly. Studies have shown that in the constitutive equation for grout, the influence of the properties of the grout on the grout flow represented by the yield shear force and viscosity can be replaced by the apparent viscosity.[22,23] Therefore, in the previous analysis, the dynamic viscosity, which represents the rheological properties of the slurry, is replaced by the apparent viscosity. The output power of the mixer is 300 W, and the maximum mixing capacity is 0.015 m^3.

5.3. Design of the Experiments. Table 3 lists the arrays of a total of 27 experiments with the above three factors. In the experimental process, first, a certain volume of silica sol solution and NaCl solution were measured, and the two were placed in an incubator for more than 30 min until the material reaches 20°C. After, the materials were mixed in a beaker and stirred in a mixer for 1 min (the speed of the mixer was 200 r/min) to ensure that the slurry was evenly mixed. The gelation test also takes place in an incubator. Then, a viscosity meter was used to assess the viscosity of the slurry at a certain time interval. When the viscosity of the slurry increases slowly, data are recorded every 1 min; when the viscosity of the slurry increases rapidly, the data are recorded every 1 s. When the viscosity reached 500 mPa·s, the slurry was stopped and the experimental data were kept and recorded.

5.4. Research Method of Fast Curing Grout in Fissure. Comparing with the cement-single slurry, silica sol as a quick-setting grout has significant spatial and temporal variation characteristics. This is because of the fact that before the grouting, two components of grout are delivered by independent grouting pipe and can be mixed inside the injection hole subsequently. The viscosity of the grout injected first is higher than that of the grout injected later. The slurry has different viscosity at different positions and times. Therefore, it is hard to be simulated using the simulation software or grouting model.

To study the effect of the time- and spatial-dependent behavior of the viscosity on the diffusion process of grouting in fissures, silica sol grout and cement−sodium silicate grout (C-S

https://doi.org/10.1021/acsomega.1c04216
ACS Omega 2021, 6, 28140−28149

Table 4. Parameters Adopted for the Generation of the Simulations under Different Conditions

grouting type	grout type	fissure width, b (mm)	radius of grouting hole, r_0 (m)	grouting rate, q (m^3/s)	grouting time, T (s)	grouting pressure, p (Pa)	equations of time-dependent behavior of the viscosity
constant-pressure grouting	silica sol	0.5, 1.0, 1.5, 2.0	0.02		60	5000, 9000, 13 000, 17 000, 21 000, 25 000	$\mu(t) = \mathrm{Exp}(33.6008\text{-}77.8550t + 48.438t^2)$
	C-S	0.5, 1.0, 1.5, 2.0	0.02		60	5000, 9000, 13 000, 17 000, 21 000, 25 000	$\mu(t) = 3.182t^{2.23} + 40$
constant-rate grouting	silica sol	2.5	0.02	0.00025	60		$\mu(t) = \mathrm{Exp}(33.6008 - 77.8550t + 48.438t^2)$
	C-S	2.5	0.02	0.00025	60		$\mu(t) = 3.182t^{2.23} + 40$

grout) were studied as examples. The improved stepwise calculation method considering the spatial and temporal variation characteristics of grout is used. The method was proposed by our research group, and the basic principle is detailed in the literature.[32] The method adopts the theory of the iterative method, and the grouted zone is divided into finite elements based on the time interval. In every time interval, the key grouting parameters, such as the penetration length, grouting pressure, and flow rate, can be calculated.

The viscosity function of silica sol was established based on the results of the previously mentioned experiment. The slurry ratio parameters were α = 30%, β = 10%, and m = 6:1, and the initial viscosity was set at 40 mPa·s.[35] The time-dependent equation of the C-S slurry viscosity is proposed in ref 23. The slurry ratio parameter is w/c = 1, C/S = 1:1, and the initial viscosity is 40 mPa·s. According to the stepwise algorithm proposed in the literature,[36] the grouting diffusion calculation program under different conditions was written and the calculation results were obtained. The calculated parameters are given in Table 4.

Table 5 lists the arrays for a total of nine experiments with two factors, including the fissure width and grouting pressure.

Table 5. Calculation Parameters under Constant Pressure

trial	fissure width, b (mm)	grouting pressure, p (Pa)
condition 1	0.5	9000
condition 2	1.0	9000
condition 3	1.5	9000
condition 4	2.0	9000
condition 5	2.0	5000
condition 6	2.0	13 000
condition 7	2.0	17 000
condition 8	2.0	21 000
condition 9	2.0	25 000

For constant-pressure grouting, fissure width values of 0.5, 1.0, 1.5, and 2.0 mm are selected. Six grouting pressure schemes, 5000, 9000, 13 000, 17 000, 21 000, and 25 000 Pa, were adopted under the test condition of a fissure aperture of 2 mm. Under the condition of constant-rate grouting, the diffusion distances of different types of grout at the same time are obviously equal. Therefore, the diffusion process of silica sol grout and C-S grout in the flat fissure under the condition of a constant rate and speed was calculated, and the pressure distribution curve in the fissure of the grouting diffusion zone was studied with emphasis. The specific calculation parameters are shown in Table 4.

AUTHOR INFORMATION

Corresponding Author

Chenghao Han − *College of Earth Science and Engineering, Shandong University of Science and Technology, Qingdao 266590, China;* orcid.org/0000-0002-4678-757X; Email: sdusthch@163.com

Authors

Weijie Zhang − *College of Earth Science and Engineering, Shandong University of Science and Technology, Qingdao 266590, China*

Fei Yang − *College of Earth Science and Engineering, Shandong University of Science and Technology, Qingdao 266590, China*

Qian Ren − *College of Earth Science and Engineering, Shandong University of Science and Technology, Qingdao 266590, China*

Ziyu Peng − *College of Earth Science and Engineering, Shandong University of Science and Technology, Qingdao 266590, China*

Fangxiao Wu − *College of Earth Science and Engineering, Shandong University of Science and Technology, Qingdao 266590, China*

Zhenyong Zhang − *College of Earth Science and Engineering, Shandong University of Science and Technology, Qingdao 266590, China; Xi'an Research Institute of China Coal Technology & Engineering Group Corp, Xi'an 710054, China*

Complete contact information is available at: https://pubs.acs.org/10.1021/acsomega.1c04216

Notes

The authors declare no competing financial interest.

ACKNOWLEDGMENTS

This study was supported by the Scientific Research Foundation of Shandong University of Science and Technology for Recruited Talents (No. 2017RCJJ030), the National Natural Science Foundation of China (Project No. 51509148), and the National Key R&D Program of China (Project No. 2017YFC0804100). The authors are extremely grateful for the financial support from these organizations.

REFERENCES

(1) Dong, S. N.; Liu, Z. X.; Zheng, S. T.; Wang, H.; Shi, Z. Y.; Shang, H. B.; Zhao, C. H.; Zheng, L. C. Technology and application of large curtain grouting water conservation mining based on macroscopic and mesoscopic characteristics of rock mass. *J. China Coal. Soc.* **2020**, *45*, 1137−1149.

(2) Pedrotti, M.; Wong, C.; El Mountassir, G.; Lunn, R. J. An analytical model for the control of silica grout penetration in natural groundwater systems. *Tunn. Undergr. Space. Technol.* **2017**, *70*, 105−113.
(3) Li, S. C.; Han, W. W.; Zhang, Q. S.; Liu, R. T.; Weng, X. J. Research on time-dependent behavior of viscosity of fast curing grouts in underground construction grouting. *Chin. J. Rock. Mech. Eng.* **2013**, *32*, 1−7.
(4) Guan, X. M.; Zhang, H. B.; Yang, Z. P.; Li, H. Y.; Lu, J. J.; Di, H. F.; Shuai, B.; Xu, C.; Wang, G. P. Research of high performance inorganic-organic composite grouting materials. *J. China Coal. Soc.* **2020**, *45*, 902−910.
(5) Zhang, H. B.; Di, H. F.; Liu, Q. B.; Hopu, C. Y.; Zheng, D. D.; Chai, H. C.; Zhou, H. F.; Liu, L.; Guan, X. M. Research and application of micro-nano inorganic grouting materials. *J. China Coal. Soc.* **2020**, *45*, 949−955.
(6) Funehag, J.; Gustafson, G. Design of grouting with silica sol in hard rock-New methods for calculation of penetration length, Part I. *Tunn. Undergr. Space. Technol.* **2008**, *23*, 1−8.
(7) Guo, H.; Li, B.; Zhang, Y.; Wang, X.; Zhang, F. Hydrophilic characteristics of soft rock in deep mines. *Int. J. Min. Sci. Technol.* **2015**, *25*, 177−183.
(8) Zheng, P. Q.; Chen, W. Z.; Tan, X. J.; Dai, Y. H. Study of failure mechanism of floor heave and supporting technology in soft rock of large deformation roadway. *Chin. J. Rock. Mech. Eng.* **2015**, *34*, 3143−3150.
(9) Li, G.; Jiang, Z.; Lv, C.; Huang, C.; Chen, G.; Li, M. Instability mechanism and control technology of soft rock roadway affected by mining and high confined water. *Int. J. Min. Sci. Technol.* **2015**, *25*, 573−580.
(10) Zhang, D. L.; Sun, Z. Y.; Song, H. R.; Fang, H. C. Water inrush evlutionary mechanisms of subsea tunnels and process control method. *Chin. J. Rock. Mech. Eng.* **2020**, *39*, 649−667.
(11) Wang, M. S.; Haungfu, M. Key problems on subsea tunnel construction. *J. Arc. Civ. Eng.* **2005**, *04*, 1−4.
(12) Butrón, C.; Gustafson, G.; Fransson, Å.; Funehag, Johan. Drip sealing of tunnels in hard rock: A new concept for the design and evaluation of permeation grouting. *Tunn. Undergr. Space. Technol.* **2010**, *25*, 114−121.
(13) Wang, K.; Wang, L. G.; Lu, Y. L.; Sun, X. K.; Zhang, K. W. Visual experimental study on the infiltration effect of cement slurry in micro-fractures. *J. China Coal. Soc.* **2020**, *45*, 990−997.
(14) Eklund, D.; Stille, H. Penetrability due to filtration tendency of cement-based grouts. *Tunn. Undergr. Space. Technol.* **2008**, *23*, 389−398.
(15) Henn, R. W.; Soule, N. C. *Ultrafine Cement In Pressure Grouting*; American Society of Civil Engineers, Academic Press: Reston, 2010; p 15.
(16) Zhang, J. P.; Liu, L. M.; Liu, C. X.; Liu, Y. B.; Wen, G. C.; Sun, D. L.; Shao, J. Mechanism and experimental study of silicon self-stress grouting reinforcement for deep fractured rock mass. *J. China Coal Soc.* **2020**, *45*, 755−765.
(17) Pan, D. J. *Permeation Law and Long-term Solidification Stability Evaluation in Loose Coal with Silica Sol Grout(D)*; China University of Mining and Technology: Xuzhou, 2018.
(18) Pan, D. J.; Zhang, N.; Zhang, C. H.; Qian, D. Y.; Han, C. L.; Yang, S. Long-Term Mechanical Behavior of Nano Silica Sol Grouting. *Nanomaterals* **2018**, *8*, No. 46.
(19) McCartney, J.; Nogueira, C. L.; Homes, D.; Zornberg, J. G. Formation of Secondary Containment Systems Using Permeation of Colloidal Silica. *J. Environ. Eng.* **2011**, *137*, 444−453.
(20) Liu, R. T. *Study on Diffusion and Plugging Mechanism of Quick Setting Cement Based Liurry in Underground Dynamic Water Grouting and Its Application(D)*; Shandong University: Jinan, 2012.
(21) Li, S. C.; Han, W. W.; Zhang, Q. S.; Liu, R. T.; Weng, X. J. Research on time-dependent behavior of viscosity of fast curing grouts in underground construction grouting. *Chin. J. Rock. Mech. Eng.* **2013**, *32*, 1−7.
(22) Zhang, Q. S.; Zhang, L. Z.; Zhang, X.; Liu, R. T.; Zhu, M. T.; Zheng, D. Z. Grouting Diffusion in a Horizontal Crack Considering Temporal and Spatial Variation of Viscosity. *Chin. J. Rock. Mech. Eng.* **2015**, *34*, 1198−1210.
(23) Zhang, W.; Li, S. C.; Wei, J. C.; Zhang, Q. S.; Liu, R. T.; Zhang, X.; Yin, H. Y. Grouting rock fractures with cement and sodium silicate grout. *Carbonates Evaporites* **2018**, *33*, 211−222.
(24) Sui, W. H.; Liu, J. Y.; Hu, W.; Qi, J. F.; Zhan, K. Y. Experimental investigation on sealing efficiency of chemical grouting in rock fracture with flowing water. *Tunn. Undergr. Space. Technol.* **2015**, *50*, 239−249.
(25) Wang, P.; Li, S. C.; Zhao, S. S.; Li, J. L.; Li, Y. Temperature Effect on Gelation Time for Nano-sized Silica Sol Grout. *J. Chin. Cer. Soc.* **2020**, *48*, 231−236.
(26) Wang, P.; Li, S. C.; Li, Y.; Feng, X. D.; Xie, C.; Wan, Z.; Wang, M. L.; Zhou, H. Y.; Ma, P. F. Experimental research on rheological and mechanical properties of nano silica sol grout. *J. Sol-Gel Sci. Technol.* **2019**, *91*, 178−188.
(27) Shen, P.; Hankins, N.; Jefferis, S. Selection of Colloidal Silica Grouts with Respect to Gelling and Erosion Behaviour. *Geosciences* **2017**, *7*, 6.
(28) Funehag, J.; Fransson, Å. Sealing narrow fractures with a Newtonian fluid: Model prediction for grouting verified by field study. *Tunn. Undergr. Space. Technol.* **2006**, *21*, 492−498.
(29) Kim, J. S.; Lee, I. M.; Jang, J. H.; Choi, H. Groutability of cement−based grout with consideration of viscosity and filtration phenomenon. *Int. J. Numer. Anal. Met.* **2009**, *33*, 1771−1791.
(30) Mohajerani, S.; Baghbanan, A.; Wang, G.; Forouhandeh, S. F. An efficient algorithm for simulating grout propagation in 2D discrete fracture networks. *Int. J. Rock Mech. Min. Sci.* **2017**, *98*, 67−77.
(31) Zhang, Q. S.; Zhang, L. Z.; Liu, R. T.; Li, S. C.; Zhang, Q. Q. Grouting mechanism of quick setting slurry in rock fissure with consideration of viscosity variation with space. *Tunn. Undergr. Space. Technol.* **2017**, *70*, 262−273.
(32) Han, C. H.; Wei, J. C.; Zhang, W. J.; Zhou, W. W.; Yin, H. Y.; Xie, D. L.; Yang, F.; Man, X. Q.; et al. Numerical Investigation of Grout Diffusion Accounting for the Dynamic Pressure Boundary Condition and Spatiotemporal Variation in Slurry Viscosity. *Int. J. Geomech.* **2021**, *21*, No. 04021018.
(33) Ming, T. *Study on Properties of Silica Sol Modified Superfine Cement Grouting Material(D)*; Wuhan University of Technology, 2018.
(34) Agapoulaki, G. I.; Papadimitriou, A. G. Rheological Properties of Colloidal Silica Grout for Passive Stabilization Against Liquefaction. *J. Mater. Civ. Eng.* **2018**, *30*, No. 04018251.
(35) Han, C. H.; Zhang, W. J.; Zhou, W. W.; Guo, J. B.; Yang, F.; Man, X. Q.; Jiang, J. G.; Zhang, C. R.; Li, Y. J.; Wang, Z.; Wang, H. Experimental investigation of the fracture grouting efficiency with consideration of the viscosity variation under dynamic pressure conditions. *Carbonates Evaporites* **2020**, *35*, 251−296.
(36) Wei, J. C.; Han, C. H.; Zhang, W. J.; Xie, C.; Zhang, L. Z.; Li, X. P.; Zhang, C. R.; Jiang, J. G. Mechanism of fissure grouting based on step-wise calculation method. *Rock. Soil. Mec.* **2019**, *40* (03), 913−925.

https://doi.org/10.1021/acsomega.1c04216
ACS Omega 2021, 6, 28140−28149